JOURNAL OF CATALYSIS 147, 379–392 (1994)

Characterization, Activity, and Adsorption/Desorption Behavior of Alkali-Promoted Molybdate Catalysts for the Oxidative Coupling of Methane

Sharon A. Driscoll, Donna K. Gardner, and Umit S. Ozkan[1]

Department of Chemical Engineering, The Ohio State University, Columbus, Ohio, 43210

Received November 27, 1993; revised January 11, 1994

$MnMoO_4$ and alkali-promoted (Li, Na, or K) $MnMoO_4$ catalysts have been examined for the methane oxidative coupling reaction. The catalysts were characterized by XRD, XPS, LRS, TPR, and TPD. The molybdate structure appeared to remain intact, although the presence of the promoter ions was found to change the TPR and TPD profiles. Increased selectivity to C_2 hydrocarbons has been observed for similar conversion levels (Driscoll, Zhang, and Ozkan, *in* "Catalytic Selective Oxidation" (S. T. Oyama and J. W. Hightower, Eds.), Vol. 523, p. 340. ACS, Washington, DC, 1993) through the addition of the alkali-promoter ions, especially potassium. Further examination of the catalysts at equal residence times revealed an increased activity due to the addition of the alkali-promoter ions, with no change in activity or selectivity when excess carbon dioxide was added to the feed. While the TPD experiments provided clues as to the nature and function of surface oxygen, laser Raman spectroscopy studies provided evidence of the existence of carbonyl groups on the surface.

INTRODUCTION

Oxidative coupling of methane has been a much investigated area since the early reports of Keller and Bhasin (2). In spite of the large volume of literature available on the subject (2–11), and in spite of some major breakthroughs, questions still remain regarding the nature of active sites, the role of oxygen, and the factors that control selectivity.

Alkali promoters have been used to change the catalytic behavior of various systems in oxidative coupling reactions (4, 5). They have been found to behave differently in different systems, acting to increase selectivity at the expense of catalytic activity over some catalysts (4, 5), while increasing both activity and selectivity in others (6). While part of the effect has been attributed to the observed decrease in catalyst surface area, additional selectivity changes have been explained in terms of the nature of the promoter ion (7, 8).

[1] To whom correspondence should be addressed.

A decrease in product oxidation due to alkali addition was given as an explanation for an observed selectivity increase during reduction/oxidation cycles by Jones *et al.* (7). The nature of the unpromoted metal oxide catalyst, the alkali metal ion used as a promoter, and the concentration of the promoter ion can all affect the activity of the catalyst. Burch *et al.* (9) have suggested that the function of alkali promoters may be to poison the sites for complete oxidation on the surface for some metal oxide catalysts, leading to an observed decrease in catalytic activity.

For alkali-promoted alkaline earth catalysts such as Li/MgO, the active site for hydrogen abstraction has been suggested as $[Li^+O^-]$ centers formed on the catalyst surface (10), with similar sites proposed for Na-promoted calcium oxide catalysts (11). Temperature programmed desorption studies of Li-promoted MgO and Na-promoted CaO led McCarty and Quinlan (12) to suggest that under reaction conditions a passive molten carbonate layer was formed on the surface of the catalyst. The active centers were said to be surface hydroxides and oxides adsorbed on the carbonate. Korf *et al.* (13) have also proposed the involvement of a carbonate layer but indicated that the active sites were generated through the decomposition of the carbonate in the presence of oxygen.

In a few studies carbon dioxide has been added to the feed gas, replacing a portion of an inert diluent, to investigate its effects on catalytic activity and selectivity in methane coupling reactions (14–19). Differences have been observed with excess carbon dioxide in the feed for some catalyst systems, and it has been suggested that competitive adsorption between carbon dioxide and oxygen may be occurring, leading to an increase or decrease in selectivity and to a decrease in the overall catalytic activity. Hutchings *et al.* (14) found the C_2 selectivity and catalytic activity to decrease reversibly for Li/MgO catalysts, returning again to the original levels when the added carbon dioxide was removed from the feed. Suzuki *et al.* (15) and Aika and Nishiyama (16, 17) investigated Sm_2O_3 and MgO through CO_2 addition, and found the selectivity to

0021-9517/94 $6.00

C_2 hydrocarbons and the formation of CO to increase. Other results have indicated that under certain conditions the addition of CO_2 can have no effect (18) or cause a catalyst to become completely inactive (19). Carbon dioxide has also been investigated for use as an oxidant by Nishiyama and Aika (20), who found that minor amounts of oxygen were required for catalyst stability.

Our work has focused on the use of alkali promoters for a simple molybdate catalyst, $MnMoO_4$, for the oxidative coupling reaction. Previous methane coupling studies using molybdates have dealt with unpromoted forms of these catalysts. A study of Na, Li, K, Mg, Ba, Mn, Co, Fe, Cu, Zn, and Ni molybdates by Kiwi *et al.* (21) showed that with the exception of $NiMoO_4$, the molybdates were stable for long periods of time under reaction conditions for oxidative coupling. The $MnMoO_4$ and K_2MoO_4 molybdates were the least selective for C_2 hydrocarbon formation. Another molybdate, $PbMoO_4$, was also studied by Carreiro *et al.* (22) at low conversion levels. We have previously reported results obtained for alkali-promoted manganese molybdate and the significantly higher selectivity obtained using the K promoter ion as compared to the unpromoted molybdate, or the molybdate promoted with Li or Na. We have examined these catalysts using isotopically labeled feed gases to study the oxygen (23) and carbon (24) transients. In this paper, we report additional characterization and kinetic results for $MnMoO_4$ and $MnMoO_4$ catalysts promoted with either Li, Na, or K for methane oxidative coupling, and the effect of excess carbon dioxide on the catalytic activity and selectivity.

EXPERIMENTAL

Catalyst Preparation and Characterization

The molybdate catalysts used in these experiments as pure $MnMoO_4$ or $MnMoO_4$ promoted by alkali metal ions were prepared in our laboratory using a technique described earlier (25). The pure $MnMoO_4$ was produced through a precipitation reaction of the metal salts. The precipitate is formed by adding a solution of ammonium heptamolybdate (Mallinckrodt) drop-wise to a solution of manganese chloride (Sigma) at 80°C. The pH of the reaction mixture was maintained at 6.0 throughout the precipitation using a pH controller (Cole Parmer, Model 5991-201), and two acid/base pumps (Masterflex, Model 7014) for the addition of dilute solutions of HCl and NH_4OH. The catalyst precursor was dried in an oven overnight at 95°C, and calcined in oxygen at 800°C for 4 h. The promoted catalysts were obtained through a wet impregnation of the molybdate with alkali carbonates (Baker) such that the atomic ratio of alkali ion to manganese was 0.01 or 0.04. The alkali carbonate was added to a slurry of manganese molybdate and water, and stirred for 4 h. A convection oven was used to drive off the water at 95°C. The promoted catalysts were also calcined for 4 h at 800°C.

These catalysts were characterized through a number of techniques. BET surface area measurements were performed with a Micromeritics 2100E Accusorb instrument using krypton as the adsorbate. X-ray diffraction (XRD) patterns were obtained using a Scintag PAD V diffractometer with CuK_α radiation as the incident X-ray source. X-ray photoelectron spectroscopy analysis was performed using a Physical Electronics/Perkin–Elmer (Model 550) ESCA/Auger spectrometer, operated at 15 kV, 20 mA. The X-ray source was MgK_α radiation (1253.6 eV). Laser Raman spectra were obtained using a Spex Triplemate spectrometer (Model 1877) using a CCD (Couple Charged Device) detector equipped with a Datamate microprocessor for data collection and processing. The 514.5-nm line of a 5-W Ar ion laser (Spectra Physics) was used as the excitation source. The laser power was 100 mW. The exposure time ranged between 10 and 30 s.

Steady-State Reaction Studies

The catalyst was packed in a 9-mm O.D. 5-mm I.D. quartz reactor, and held in place by a quartz wool plug at the entrance and a quartz frit at the exit. The diameter of the reactor was decreased to 2 mm at the end of the catalyst bed to decrease the residence time in the heated zone. The total surface area in the reactor was kept constant for all runs at 0.1 m^2. The catalyst was mixed with enough powdered quartz to produce a bed length of 1.5 cm.

Three different types of steady-state experiments have been performed. Our previous experiments (1) examined the catalytic selectivity for ethane and ethylene production at equal conversion levels for both the 1 and 4% promoter ion concentration. Variations in catalytic activity and selectivity were also examined at equal residence time. We have further examined the catalysts prepared with 1% promoter ion concentration in a set of experiments at equal residence times by replacing a portion of the feed gas with carbon dioxide and comparing the results obtained with and without excess carbon dioxide in the feed.

The feed used for these experiments was a mixture of 40% methane, 20% oxygen, and 40% nitrogen. The methane coupling reaction was studied at 700°C and atmospheric pressure. When comparisons were based on equal conversion levels, the flow rate was varied to keep conversion of methane constant (near 10%) for each of the catalysts. For studies based on equal residence time, the flow rate was set at 10.6 cm^3(STP)/min. The feed for the excess carbon dioxide experiments was changed such that half of the inert nitrogen was replaced by carbon dioxide. The

products were separated and analyzed using an automated gas chromatograph (HP 5890 II). A thermal conductivity detector (TCD) was used to analyze for O_2, N_2, CO, CH_4, HCHO, C_2H_6, and C_2H_4, with a flame ionization detector (FID) also used to quantify the C_2 hydrocarbon concentrations.

Temperature Programmed Reduction and Desorption

The temperature programmed system was built in-house, and was used for both temperature programmed reduction (TPR) and desorption (TPD) experiments. The sample was placed in a quartz cell, with quartz wool plugs located at the bottom of the catalyst bed and at the top of the tube to hold the catalyst in place. The cell was heated by a furnace (Hoskins Manufacturing Company), with a chromel–alumel type K thermocouple (Omega) placed in the furnace at the same depth as the sample bed. The temperature was controlled and displayed by a TECO-SIGMA temperature controller (Model MDC10-RS232). Additional insulation at the top of the furnace helped maintain isothermal conditions over a large portion of the furnace. Helium was used as both the carrier and reference gas for the thermal conductivity detector (TCD). The flow rates were maintained by mass flow controllers (Tylan Model FC-280) and displayed on a read-out box (Tylan Model RO-28). A Zenith data systems computer was used to program the temperature controller and collect the TCD signals. The off gas was also analyzed on-line by a mass spectrometer (HP 5989A MS engine).

The TPR profiles were obtained by heating samples (50 mg) at a rate of 5°C per minute from 50 to 950°C. The temperature was then held at 950°C until the reduction was completed. The reducing gas was 6% H_2 in N_2, and the flow rate was 60 cm^3(STP)/min. The TCD reference gas was changed to nitrogen for the TPR experiments. Temperature programmed desorption studies were used to examine the interaction between various gases with the catalyst surface. In one set of experiments, the surface of the catalysts exposed to the atmosphere under ambient conditions was analyzed by performing the TPD after degassing the catalyst through evacuation at 200°C. This pretreatment method was also used prior to adsorption of methane, carbon monoxide, carbon dioxide, and oxygen in TPD studies. Following the pretreatment, the catalysts were cooled to room temperature and exposed for 2 h to the flowing adsorbate gas. The adsorbate was flushed from the system with helium prior to heating. The samples were heated from 25 to 850°C at a rate of 15°C/min and held at 850°C for 30 min.

An additional *in situ* pretreatment was also used to examine the catalysts for methane adsorption/temperature programmed desorption. The catalyst was calcined *in situ* under oxygen flow at 700°C for 4 h. It was then cooled in oxygen flow and flushed with helium prior to starting the methane flow. The methane flow continued for 2 h, followed by flushing the system with helium before beginning the TPD.

RESULTS

Surface Area Analysis

The surface areas of the promoted catalysts were found to decrease due to the presence of the promoter ion, ranging from 0.19 to 0.3 m^2/g as compared to 0.46 m^2/g for the unpromoted $MnMoO_4$ catalyst.

X-Ray Diffraction

The X-ray diffraction patterns obtained for the alkali-promoted catalysts revealed only changes in the peak widths and intensities as compared to the unpromoted $MnMoO_4$, with no new phases detected.

X-Ray Photoelectron Spectroscopy (XPS)

Pre- and postreaction analysis of the catalyst samples revealed no major differences in the observed binding energies of the alkali-promoted catalysts. The presence of sodium and potassium on the catalyst surface was verified by XPS, with no lithium detected. Postreaction analysis showed a downward shift of about 0.4–0.5 eV in the $Mo3d_{3/2}$ and $Mo3d_{5/2}$ binding energies for $K/MnMoO_4$ as compared to prereaction analysis. No shifts were observed for the $Li/MnMoO_4$ or the $Na/MnMoO_4$. Additional details have been previously reported (1).

Laser Raman Spectroscopy

Catalyst characterization studies showed the molybdate structure to remain intact after incorporation of the alkali promoter ions. The Raman spectra in Fig. 1 show that in the wavenumber region 800 to 1000 cm^{-1} the Raman features do not change for the promoted catalysts. Major bands are observed at 930, 941, 881, and 822 cm^{-1}. However, at 966 cm^{-1} an additional minor peak was observed for the Li-promoted sample, as seen in Fig. 2. This peak was not present in the uncalcined $Li/MnMoO_4$ catalyst, but formed during the calcination process. Raman spectra of lithium molybdate (GFS Chemicals), lithium carbonate (Baker), and lithium oxalate (Matheson Coleman & Bell) were obtained for comparison. The band seen over the promoted sample could not be attributed to any of these compounds, although lithium molybdate did exhibit a minor peak at approximately the same wavenumber. The profiles obtained for the Li-promoted manganese molybdate, lithium carbonate, lithium molybdate, and lithium oxalate are presented in Fig. 3.

Additional Raman analysis was performed by focusing

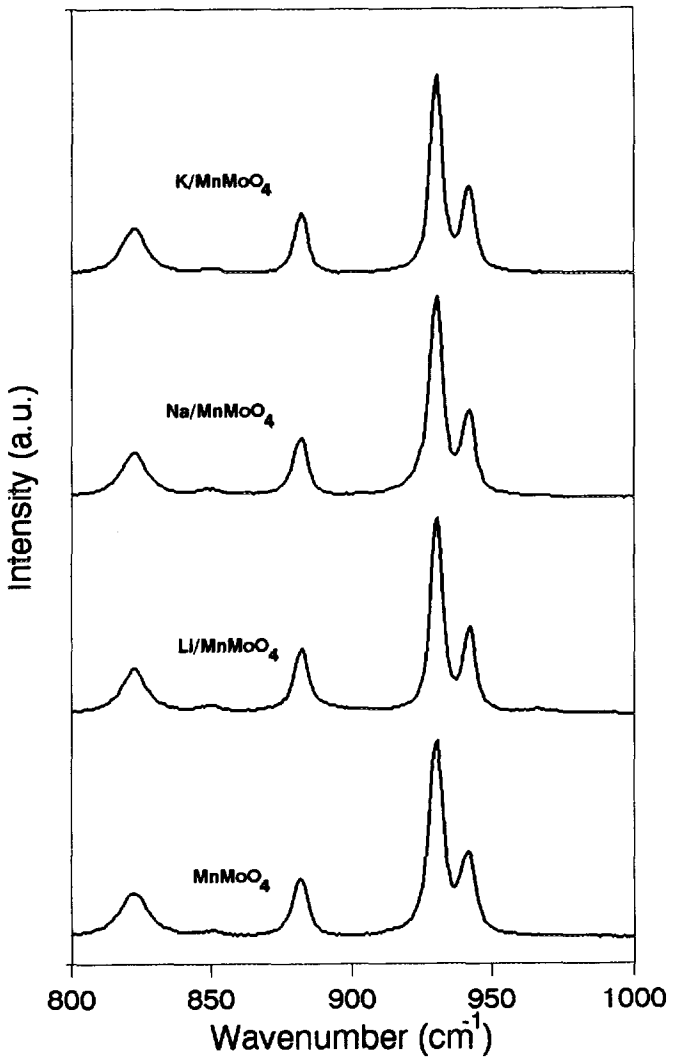

FIG. 1. Laser Raman spectra of unpromoted and alkali-promoted $MnMoO_4$ catalysts (800–1000 cm^{-1}).

on the 1000–2000 cm^{-1} wavenumber region. Figures 4, 5, and 6 show the Raman spectra of the promoted and unpromoted $MnMoO_4$ catalysts in the 1000–1400, 1400–1700, and 1700–2000 cm^{-1} wavenumber ranges, respectively. Similar spectra were obtained over the same wavenumber regions for the carbonate salts of the alkali metals that were used as promoters in this study (Figs. 7–9). The alkali carbonates exhibit a very strong band in the 1050–1100 cm^{-1} region, as seen in Fig. 7. The band positions are 1064, 1084, and 1088 cm^{-1} for potassium, sodium, and lithium, respectively. When the same region is examined over the catalyst samples (Fig. 4), there is no clear evidence of the corresponding alkali carbonates on the molybdates. Although $K/MnMoO_4$ shows a weak band at 1060 cm^{-1}, what is more striking is a broad feature in the 1110–1140 cm^{-1} range. When examined closely, a similar feature is observed over the other samples, but the intensity is much lower. In the 1400–1700 cm^{-1} region (Fig. 8), K_2CO_3 exhibits a strong band at 1404 cm^{-1} with two shoulder bands at each side. There is also a well-defined feature at 1506 cm^{-1}. The sodium carbonate spectrum shows two bands in this region, not completely resolved, at 1426 and 1435 cm^{-1}. Li_2CO_3, on the other hand, has a weak band at 1412 cm^{-1} and a sharp band at 1461 cm^{-1}. The molybdate samples do not show any of the bands that were seen in the carbonate samples in the same region (Fig. 5). Instead there is a weak band in the 1545–1555 range for all of them. In the 1700–2000 cm^{-1} region (Fig. 6), the catalyst samples show three main Raman features—a broad band in the 1740–1755 cm^{-1} range and a doublet between 1800 and 1900 cm^{-1}. The doublet shows the best resolution and the highest intensity over the $K/MnMoO_4$ catalyst. The carbonates do not show these features in the same range.

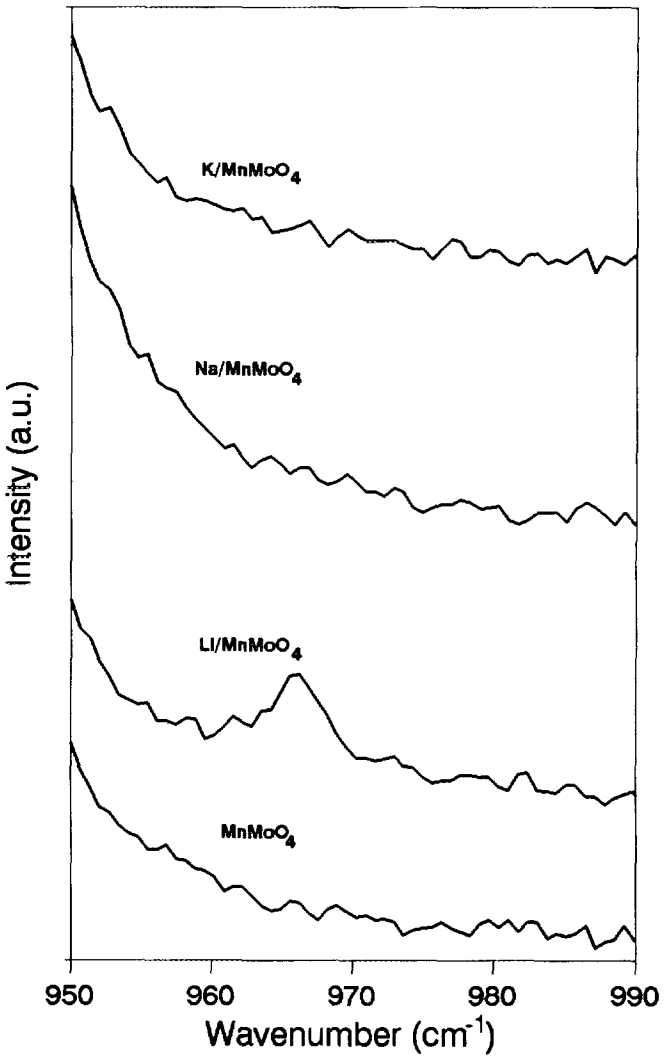

FIG. 2. Laser Raman spectra of unpromoted and alkali-promoted $MnMoO_4$ catalysts (950–990 cm^{-1}).

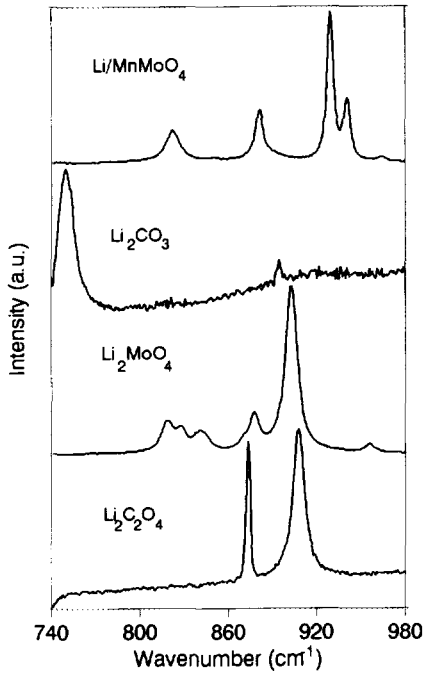

FIG. 3. Laser Raman spectra of $Li/MnMoO_4$, Li_2CO_3, Li_2MoO_4, and $Li_2C_2O_4$.

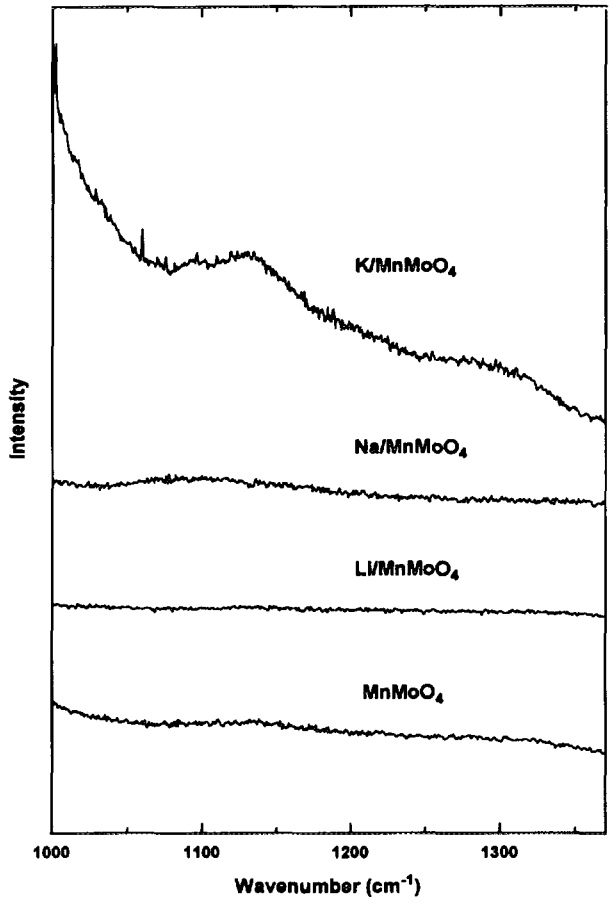

FIG. 4. Laser Raman spectra of unpromoted and alkali-promoted $MnMoO_4$ catalysts (1000–1350 cm^{-1}).

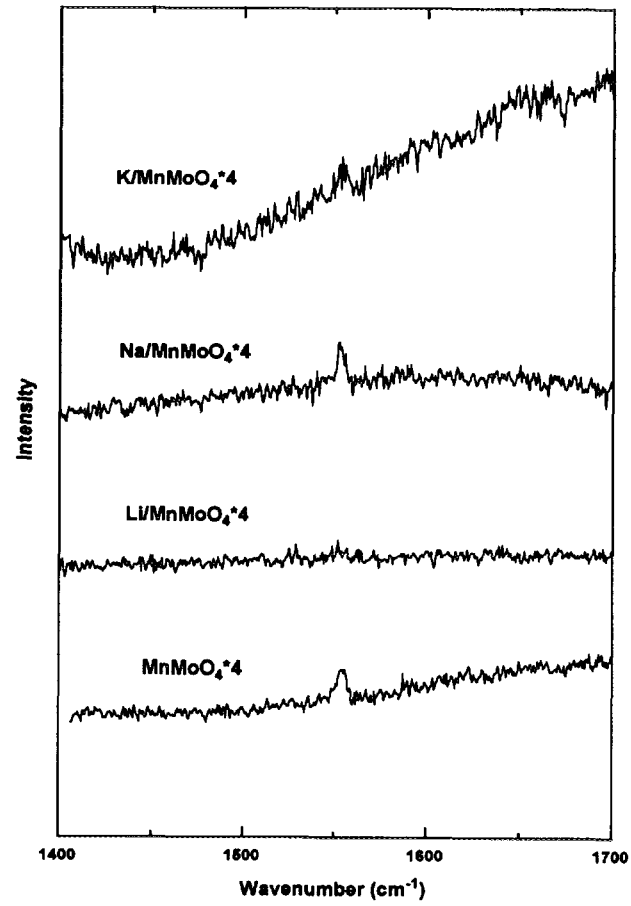

FIG. 5. Laser Raman spectra of unpromoted and alkali-promoted $MnMoO_4$ catalysts (1400–1700 cm^{-1}).

Steady-State Experiments

The conversion obtained for an empty reactor, or for a reactor filled with quartz chips, was found to be minimal under most of the conditions used in this study. To examine the effect of excess carbon dioxide on the homogeneous reaction at a quantifiable conversion level, the flow rate was decreased to one-half that used in the studies performed at a constant flow rate (~5 cm^3(STP)/min as compared to 10.6 cm^3(STP)/min). Under these conditions, using the carbon dioxide-free feed a conversion of approximately 0.5% was obtained using quartz powder in the reactor. The major products of the homogeneous reaction were C_2H_6 and formaldehyde, with detectable but minor amounts of CO_x formed. For the CO_2-enriched feed, there was no observable difference in product formation in the blank run.

The addition of a promoter ion to manganese molybdate affected the product distribution at equal conversion levels in favor of partial oxidation products as has previously been reported (1). Shown in Fig. 10 are the selectivity

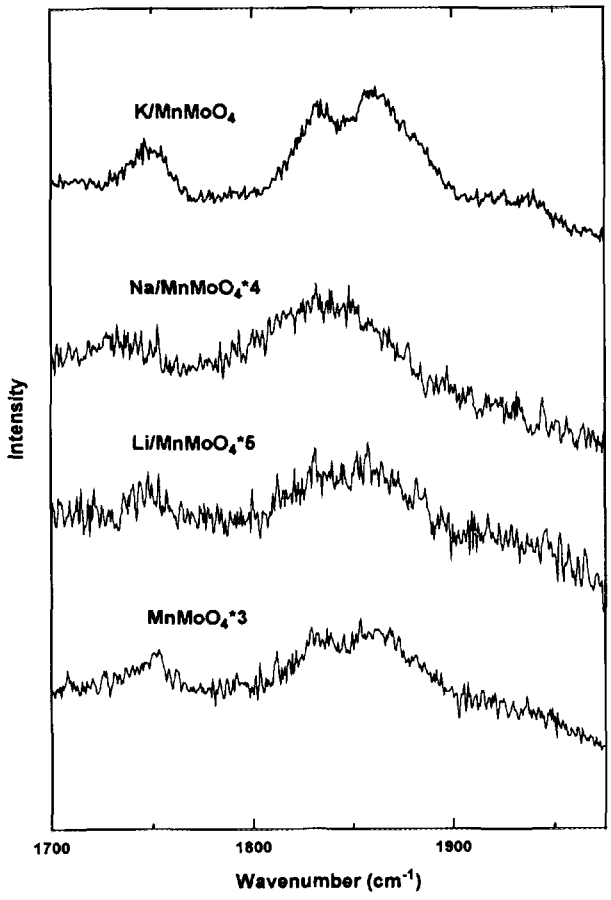

FIG. 6. Laser Raman spectra of unpromoted and alkali-promoted $MnMoO_4$ catalysts (1700–2000 cm^{-1}).

results obtained for each of the catalysts at a constant conversion level of 10%. The selectivity to C_2 hydrocarbon formation was found to increase in the order of K > Na > Li > $MnMoO_4$. The 1% $K/MnMoO_4$ catalyst was found to be the most selective catalyst studied for C_2 production, with the 4% $K/MnMoO_4$ catalyst only slightly less selective. The selectivity to CO was found to be the highest for the 1% $Li/MnMoO_4$ and unpromoted $MnMoO_4$, and only a slightly lower selectivity was observed for the Na-promoted and 4% Li-promoted catalysts. The K-promoted catalyst exhibited a much lower selectivity to CO, with the 1% loading giving approximately one-half, and the 4% loading giving only about one-third, of the selectivity obtained over unpromoted $MnMoO_4$. The selectivity of the catalysts to carbon dioxide is shown to vary with the promoter ion concentration as the 1% loading level produces consistently lower amounts of carbon dioxide than the 4% loading. The addition of Li and Na promoters was seen to increase the HCHO selectivity, with the largest increase observed over 1%$Na/MnMoO_4$, followed by 4% and 1% Li/$MnMoO_4$ catalysts. There was no increase in HCHO selectivity due to addition of the K promoter.

Excess Carbon Dioxide in the Feed

In our study, the catalytic activity of $MnMoO_4$ catalyst improved with the addition of promoter for equal residence times in each case, as shown in Table 1, with the methane conversion increasing in the order of Na > Li > K > $MnMoO_4$. $K/MnMoO_4$ remained as the most selective catalyst for C_2 hydrocarbons for both equal conversion and equal residence time comparisons.

As seen in Table 1, the addition of carbon dioxide to the feed for the methane coupling reaction did not appear to have a significant effect on the product distribution or the catalytic activity of any of the catalysts examined.

Temperature Programmed Reduction

The results from the TPR experiments using hydrogen as the reducing agent were reported earlier (1). The TPR profiles were similar for all four catalysts, showing two main peaks, with some differences in temperature maxima. X-ray diffraction was used to determine the nature

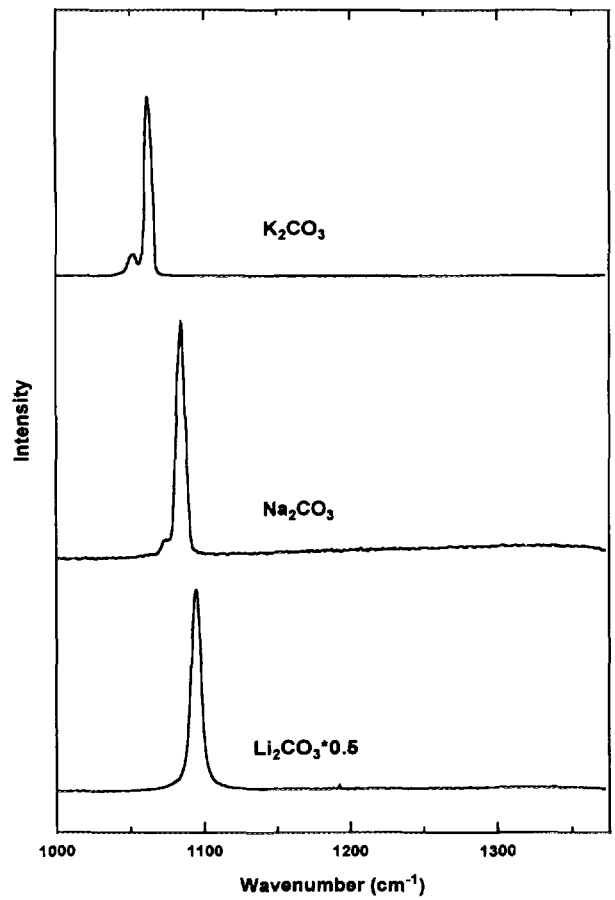

FIG. 7. Laser Raman spectra of alkali carbonates (1000–1350 cm^{-1}).

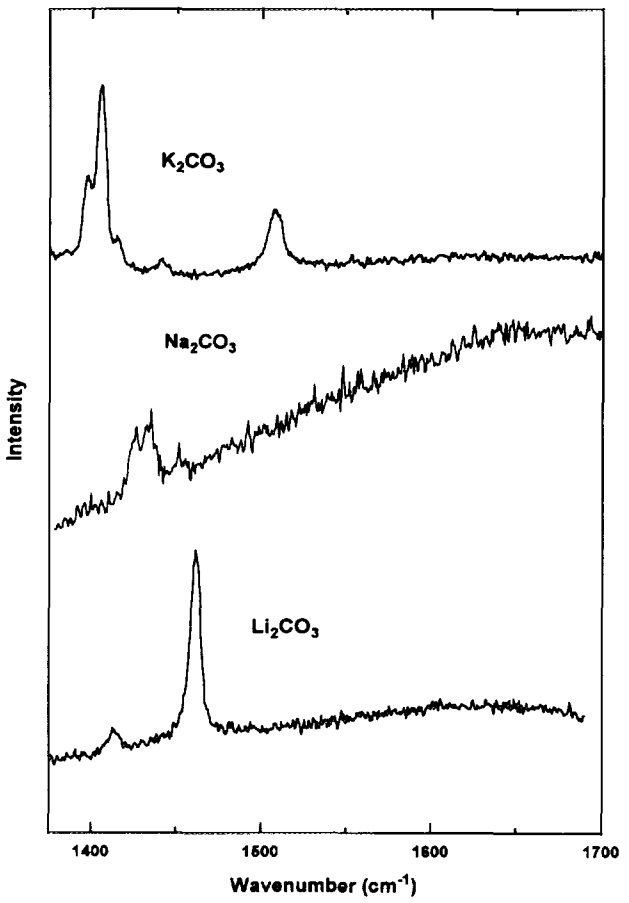

FIG. 8. Laser Raman spectra of alkali carbonates (1400–1700 cm^{-1}).

of the reduction intermediates and the final form. To obtain the TPR intermediates for each of the samples, the TPR experiment was repeated and terminated right after the first reduction peak. At the appropriate time, the hydrogen flow was stopped and the sample was quenched under nitrogen flow. The reduction process was found to be identical for each of the catalysts, with the intermediate crystal structure identified using XRD as $Mn_2Mo_3O_8$. The second peak represents the further reduction of $Mn_2Mo_3O_8$ to MnO and Mo. The total hydrogen consumption for all samples was comparable, and was in agreement with the theoretical value of 13.96 mmol/g assuming the final species to be MnO and Mo. The hydrogen consumption obtained through integration of the first peak for each catalyst was also in good agreement with the amount needed for the formation of the proposed reduction intermediate, $Mn_2Mo_3O_8$.

Temperature Programmed Desorption

Figure 11 shows desorption profiles obtained from "blank" catalyst samples after a pretreatment which consisted of degassing under vacuum at 200°C for 2 h. These samples had been stored in the laboratory after initially being calcined under oxygen flow, and were thus exposed to the atmosphere under ambient conditions. The evolved gas analysis by mass spectrometry revealed that the alkali-promoted catalysts desorbed both oxygen (m/e = 32) and carbon dioxide (m/e = 44) during the temperature programmed desorption experiment, while the unpromoted $MnMoO_4$ catalyst desorbed only carbon dioxide. The most intense CO_2 desorption peaks were at 420, 500, 450, and 640°C for the Li-, Na-, and K-promoted catalysts, and unpromoted $MnMoO_4$, respectively. Each of the carbon dioxide profiles appeared to contain a number of unresolved or partially resolved peaks. The corresponding oxygen profiles revealed two distinct desorption peaks for the Li- and K-promoted catalysts, and one broad desorption peak for the Na-promoted catalyst. The temperatures corresponding to the first oxygen peaks were at 700, 800, and 530°C for the $Li/MnMoO_4$, $Na/MnMoO_4$, and the $K/MnMoO_4$ catalysts, respectively. The second oxygen desorption peak seen for the $K/MnMoO_4$ was much smaller than the earlier peak, and the temperature

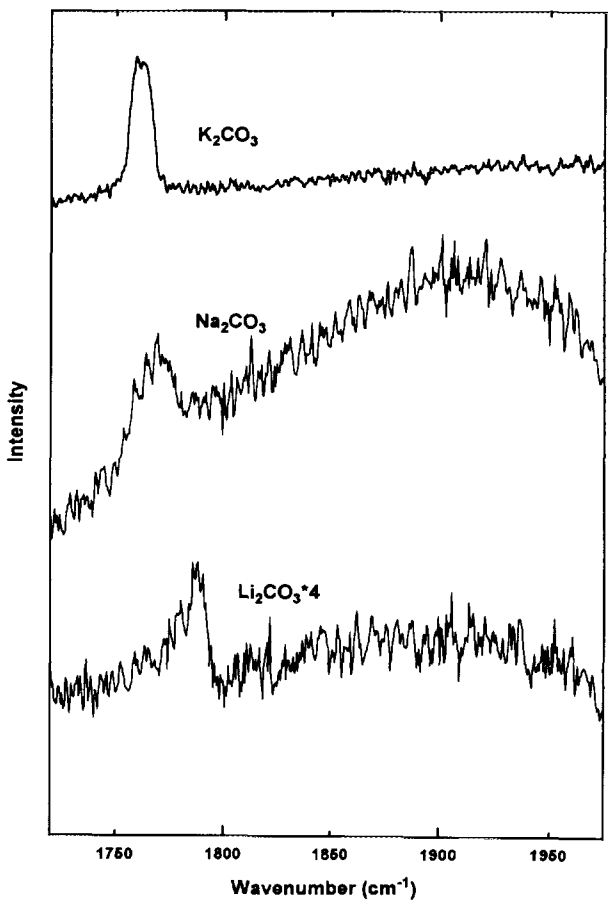

FIG. 9. Laser Raman spectra of alkali carbonates (1700–2000 cm^{-1}).

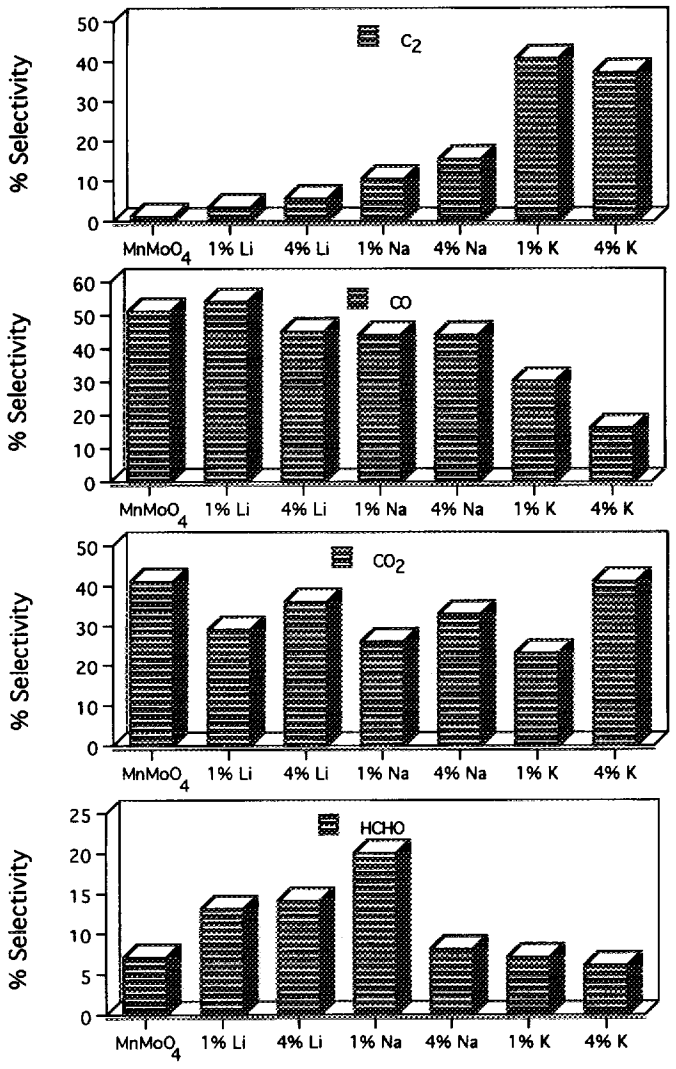

FIG. 10. Variation in selectivities at a constant conversion level of 10% for unpromoted and alkali-promoted $MnMoO_4$.

of the peak was 825°C. For the Li/$MnMoO_4$ catalyst, the second oxygen peak was of similar width and intensity as the first peak, and the maximum occurred during the isothermal portion of the TPD at 850°C. Additional catalyst samples were run without pretreatment, and again both oxygen and carbon dioxide were detected during the TPD that were nearly identical to the profiles obtained over degassed samples.

The temperature programmed desorption profiles obtained after exposure of the degassed sample to carbon monoxide at room temperature for 2 h are presented in Fig. 12. The oxygen desorption profiles are not included as there were no oxygen desorption peaks detected. The major desorption species was found to be carbon dioxide. While there may have been some carbon monoxide evolved, interference from the background nitrogen made the $m/e = 28$ signal, which also corresponds to CO, difficult to analyze. The desorption of carbon dioxide for all of the catalysts studied began between 250 and 300°C, and continued past the end of the desorption experiment. The main feature in the desorption profile obtained from the unpromoted $MnMoO_4$ was a fairly well resolved peak that began at about 600°C and intensified to a maximum at 710°C. The Li-promoted sample exhibited a single intense carbon dioxide desorption peak that appears to be superimposed on a number of broad features, with the maximum corresponding to a temperature of 425°C. The Na-promoted catalyst contains a small, sharp peak at 310°C, but the main peak maximum occurs at 550°C and appears to have a shoulder on the lower temperature side. For the K-promoted catalyst there appear to be two relatively unresolved peaks, with the more intense carbon dioxide peak desorbing at about 500°C and the less intense peak desorbing at about 450°C.

The temperature programmed desorption profiles obtained after exposure of the degassed sample to methane are presented in Fig. 13. Again, no oxygen desorption

TABLE 1

Effect of CO_2 on Activity and Selectivity of Unpromoted and Alkali-Promoted (1%) Manganese Molybdate Catalyst

Catalyst	Diluent	CH_4 conv (%)	O_2 conv (%)	C_2 yield (%)	Selectivity (%)			
					C_2	CO_2	CO	HCHO
$MnMoO_4$	N_2	3.3	10	0.08	2.4	27	52	18
	CO_2	3.3	10	0.09	2.7	23	55	19
Li/$MnMoO_4$	N_2	6.4	16	1.50	24	15	39	22
	CO_2	6.0	15	1.37	23	15	40	21
Na/$MnMoO_4$	N_2	9.8	28	1.87	19	21	42	19
	CO_2	10.4	28	1.61	19	23	42	18
K/$MnMoO_4$	N_2	5.4	12	2.37	43	22	22	13
	CO_2	5.5	12	2.47	42	22	23	13

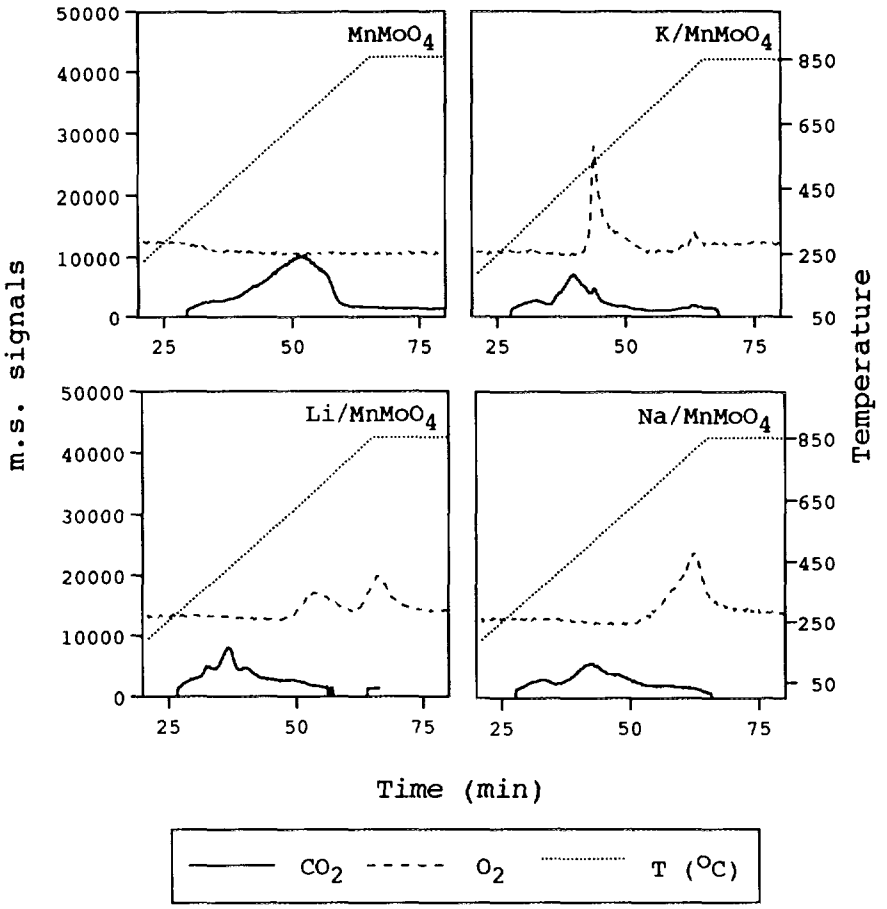

FIG. 11. Temperature programmed desorption profiles of $MnMoO_4$ and alkali-promoted $MnMoO_4$ catalysts exposed to ambient conditions.

peaks were detected, and in each case the main species desorbing was found to be carbon dioxide. There was no signal corresponding to methane, $m/e = 15$, for any of the catalysts during the temperature programmed desorption. The main features discussed above for the desorption profiles resulting from carbon monoxide adsorption are still present for methane desorption. In fact, the temperature corresponding to the most intense desorption peak for $MnMoO_4$ remained 710°C. The major desorption peak for the $Li/MnMoO_4$ catalyst shifted to a slightly higher temperature, 460°C, while the larger peak for the $Na/MnMoO_4$ appears to have decreased slightly in intensity and shifted so that the temperature corresponding to the peak maximum was 580°C. The most significant change was observed in the $K/MnMoO_4$ catalyst. It appears that there are still two unresolved peaks, but they are now of similar intensity, and the corresponding temperatures shifted down to 400 and 440°C. Another important feature of the TPD experiment over $K/MnMoO_4$ following methane adsorption was the fairly sharp water desorption peak that evolved at about the same temperature that the first CO_2 peak evolved.

When TPD experiments were performed over the degassed samples after exposing them to oxygen and to carbon dioxide, the TPD profiles obtained were almost identical to those that were seen with no adsorption step. For each catalyst there were only minor changes in both the overall intensity and in the relative intensity of the desorption profiles. The general shape and the location of the peaks did not change, and no additional oxygen or carbon dioxide desorption peaks occurred during the respective experiments. The *in situ* calcination prior to methane adsorption resulted in no methane or carbon dioxide peaks below 850°C. This was true for both the high-temperature and low-temperature adsorption experiments.

DISCUSSION

Unpromoted $MnMoO_4$ and $MnMoO_4$ promoted with Li, Na, and K have been examined for the methane coupling reaction. The significant differences we have observed in the promoted catalysts compared to the unpromoted $MnMoO_4$, and among the alkali-promoted catalysts

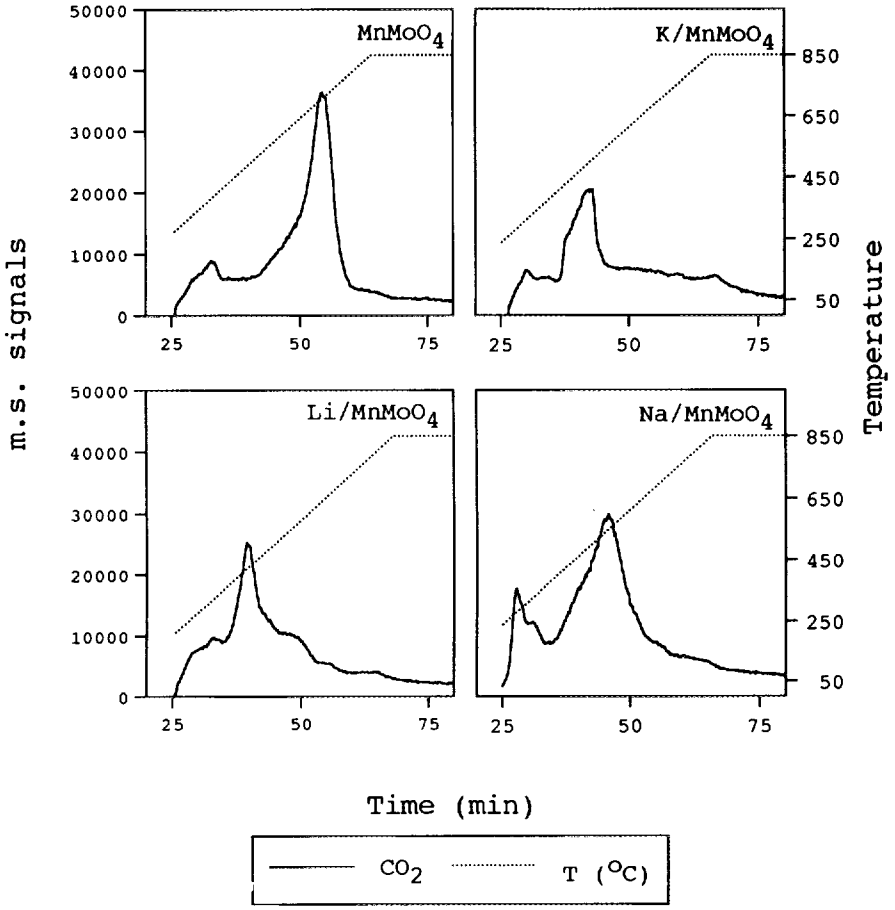

FIG. 12. Temperature programmed desorption profiles of $MnMoO_4$ and alkali-promoted $MnMoO_4$ catalysts following room temperature carbon monoxide adsorption.

through activity and selectivity measurements and isotopic labeling studies, have been further examined through additional characterization experiments. With the exception of the Li-promoted catalyst, which exhibited a unique feature at 966 cm^{-1} when examined using laser Raman spectroscopy, it appears that it is mainly the surface of the manganese molybdate catalyst that was modified due to the addition of the promoter ions, as no new bulk phases were detected. While the surface modification appears to strongly influence the catalytic properties and the observed catalytic activity and selectivity for the methane coupling reaction, the bulk manganese molybdate structure seems to remain intact for the alkali-promoted catalysts. In the case of $Li/MnMoO_4$, it is conceivable that the Li atoms are incorporated into the lattice without significantly distorting the lattice structure, but possibly creating some defects.

The volatility of alkali metals, especially Li, is a legitimate concern when they are used as promoters. The post-reaction characterization of the catalysts performed using laser Raman spectroscopy and X-ray photoelectron spectroscopy did not show any differences compared to that of the fresh catalysts. Also, keeping the catalysts on-line for more than 24 h did not show any activity changes. However, it is difficult to rule out the possibility of promoter loss if the catalysts are kept on-line for much longer periods.

Exposure of the catalysts to the atmosphere under ambient conditions appears to result in the formation of highly stable surface species that lead to carbon dioxide elution during a temperature programmed desorption experiment over degassed samples. These species do not appear to change after being exposed to oxygen or to carbon dioxide as similar TPD profiles were obtained for the degassed samples, for samples exposed to either carbon dioxide or oxygen following degassing, and for samples with no pretreatment at all.

The laser Raman spectra of the samples obtained in the 1000–2000 cm^{-1} range provide some important clues as to the nature of the surface. Since one of the possibilities

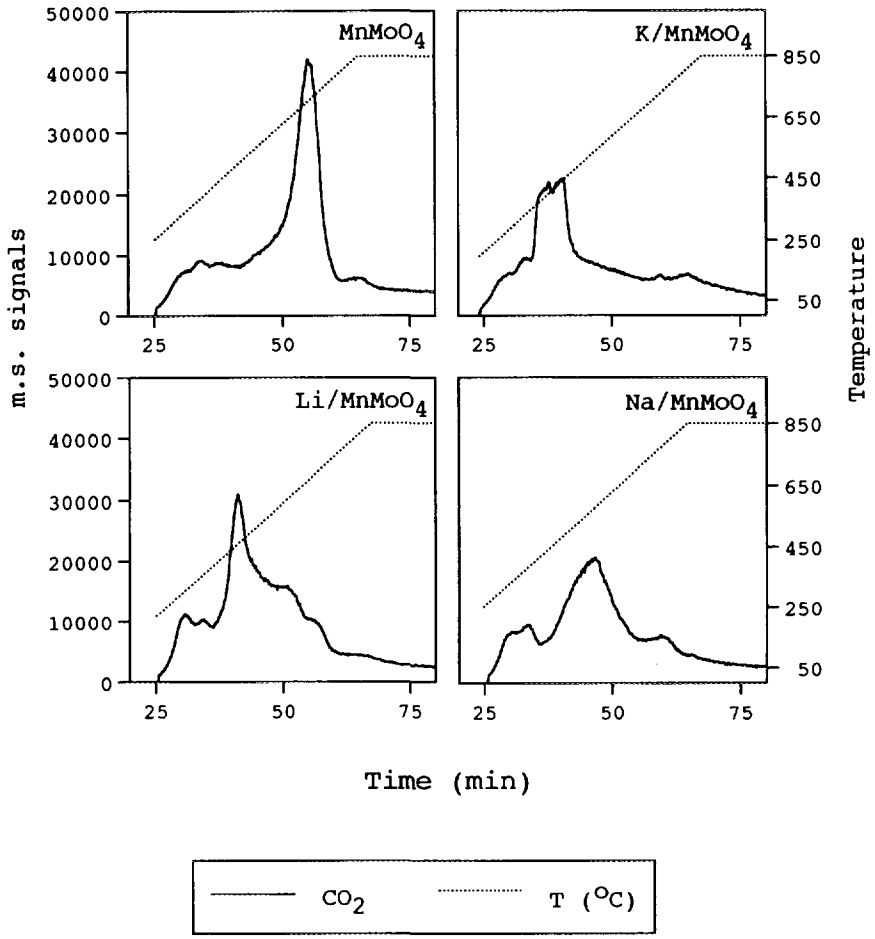

FIG. 13. Temperature programmed desorption profiles of $MnMoO_4$ and alkali-promoted catalysts following room temperature methane adsorption.

is the formation of an alkali carbonate layer on the surface, a comparison to pure carbonates is presented. As seen in Fig. 7, all three carbonates exhibit a sharp band in the 1050–1100 cm^{-1} range, which is associated with the in-phase CO_3 stretch (28). This band is either completely nonexistent over the catalyst samples or appears as a very weak feature, as in the case of $K/MnMoO_4$. What is more interesting is the appearance of some new features over the catalyst samples in the 1700–1900 cm^{-1} region in the form of one broad band and a doublet which do not appear in the alkali carbonates. Another important aspect of these findings is the fact that these features appear to be most pronounced over $K/MnMoO_4$ catalysts. These observations suggest the presence of carbonyl species on the surface. It also appears that these are surface-coordinated species and are different from simple alkali carbonates.

The carbonyl species also seem to be closely associated with the methane activation behavior of the catalysts, as seen in the TPD studies performed over samples that were calcined *in situ* and then exposed to methane either at room temperature or at reaction temperature. The TPD profiles that followed showed no methane or carbon oxides desorbing from the surface, indicating that once the carbonyl species on the surface are decomposed the surface loses the active sites for methane activation or adsorption. Also, the fact that the most intense Raman features that signal the presence of these species is seen over the most selective catalyst suggests that these sites may be responsible for formation and/or retention of methyl radicals without further oxidizing them immediately. Whether the continued presence of surface carbonyl species under reaction conditions provide the catalytic activity or the carbonyl species act as precursors to some other active sites at reaction temperature is not clear at this point. Formation of active sites due to decomposition of carbonate species has been suggested earlier by Korf *et al.* (13). If the latter case happens to be true, the low activity and selectivity of the unpromoted catalyst can be

explained by the much higher desorption temperature for carbon dioxide over this catalyst, signaling a more stable form of the carbonyl species which does not transform into the "active sites" even at reaction temperature.

The presence of oxygen desorption peak(s) during TPD of the alkali-promoted catalysts for each of the cases mentioned above and the lack of any oxygen desorption peaks for the unpromoted $MnMoO_4$ for those same experiments may help explain the differences observed between the catalysts in terms of selectivity. The oxygen desorption profile for $K/MnMoO_4$ contains a sharp, intense oxygen desorption peak that occurs at 530°C, while for the Li-promoted catalysts no oxygen desorption occurs below 600°C, and for the Na-promoted catalyst no oxygen desorption occurs below 700°C. It may be the availability of surface-adsorbed oxygen on the Li- and Na-promoted catalysts which provide a much higher methane conversion activity although most of this activity is for oxidation products. The relatively low abundance of adsorbed oxygen over $K/MnMoO_4$ under reaction conditions, on the other hand, may be allowing the methane, once activated, to couple and form C_2 products. When the surface was exposed to methane or carbon monoxide at room temperature, there was no oxygen desorption from the surface indicating that the adsorbate gases actually reacted with the surface. This is also supported by the desorption of mainly carbon dioxide as opposed to significant desorption of methane or carbon monoxide. It appears the oxygen observed in the desorption profiles obtained for the degassed samples is highly reactive and is readily utilized in the formation of carbon dioxide during desorption.

Isotopic labeling studies performed using labeled oxygen have found differences in the interaction of the catalysts with gas-phase oxygen (23). In these studies, the feed stream is switched from the unlabeled gas mixture to labeled gas mixture without perturbing the steady state of the system. Hence, the isotope transients are followed at steady-state reaction conditions (23). Isotopic exchange with $^{18}O_2$ showed that only the K-promoted catalyst was able to produce significant amounts of cross-labeled oxygen, $^{16}O\ ^{18}O$, during $^{16}O_2/^{18}O_2$ switching experiments, although the Na- and Li-promoted catalysts formed cross-labeled oxygen only in minor amounts. These observations seem to agree with the findings of the TPD studies in that the adsorbed oxygen which stays on the surfaces of Li- and Na-promoted catalysts exchanges with molecular oxygen to give doubly unlabeled O_2, whereas, over the $K/MnMoO_4$ gas phase oxygen exchanges with a less reactive form of oxygen, which is a conceivable part of the lattice, giving rise to cross-labeled oxygen.

Under reaction conditions, all catalysts continued to show reaction products containing unlabeled oxygen in significant quantities, but the K-promoted catalyst showed the fastest decline in ^{16}O incorporation into all products except molecular oxygen (23). Figure 14 shows ^{16}O and ^{18}O incorporation rates into the products during the first 16 min after the isotopic switch. As seen in the figure, the ^{16}O incorporation rate into products remains quite high over Li- and Na-promoted catalysts, while it decays quite rapidly over $K/MnMoO_4$. Although the normalized rates do not reveal much of a difference between the unpromoted catalyst and those that are promoted with Li and Na, the absolute rates show that the ^{16}O incorporation rate for $Li/MnMoO_4$ and $Na/MnMoO_4$ is more than twice as high as for the unpromoted $MnMoO_4$. Also, the ^{16}O incorporation rate over Li- and Na-promoted $MnMoO_4$ is more than six times higher than the rate seen over $K/MnMoO_4$ 15 min after the switch. When one considers the high percentage of unlabeled oxygen that was incorporated into the products long after the gas phase was completely flushed of the unlabeled oxygen feed, it appears that there is a fast rate of diffusion of lattice oxygen from the bulk of the solid to the surface over Li- and Na-promoted catalysts. More than 95% of water formed over these catalysts, for example, remains unlabeled even 14 min after the feed oxygen is switched from unlabeled to labeled oxygen. The replenishment of the surface over the $K/MnMoO_4$, however, appears to be slower compared to the other two promoted catalysts. One possible explanation for this observation is that the relatively small size of Li and Na atoms may allow them to be incorporated into the lattice, leading to a higher oxygen mobility by way of possible defect structures. Due to their relatively larger size, especially in comparison to Mn^{+2} present in $MnMoO_4$, K ions may remain mostly on the surface, possibly in the form of some carbonyl species.

The isotopic labeling studies using a $^{12}CH_4/^{13}CH_4$ switch indicated no strong adsorption of carbon dioxide on the catalyst surface (24), but carbon monoxide and C2 species were found to remain on the surface of the K-promoted catalyst considerably longer. The longer residence time of the ^{12}CO, $^{12}C_2H_6$, and $^{12}C_2H_4$ on the surface of the $K/MnMoO_4$ may indicate a longer "surface life" for methyl radicals without undergoing further oxidation. The longer residence time may then allow the radicals to desorb and couple, or to react further to form CO.

It should also be noted that following CO adsorption and methane adsorption the TPD profiles were quite similar for both $Li/MnMoO_4$ and $Na/MnMoO_4$. However, the two TPD profiles obtained after CO adsorption and after CH_4 adsorption were significantly different for $K/MnMoO_4$. Another important feature of the TPD experiment after the CH_4 adsorption was that there were significant amounts of H_2O desorbing at the same temperature where the main CO_2 desorption took place. These observations also support the suggestion that methane stays on $K/MnMoO_4$ surface as methyl radicals long enough to desorb and couple, whereas with the other catalysts the

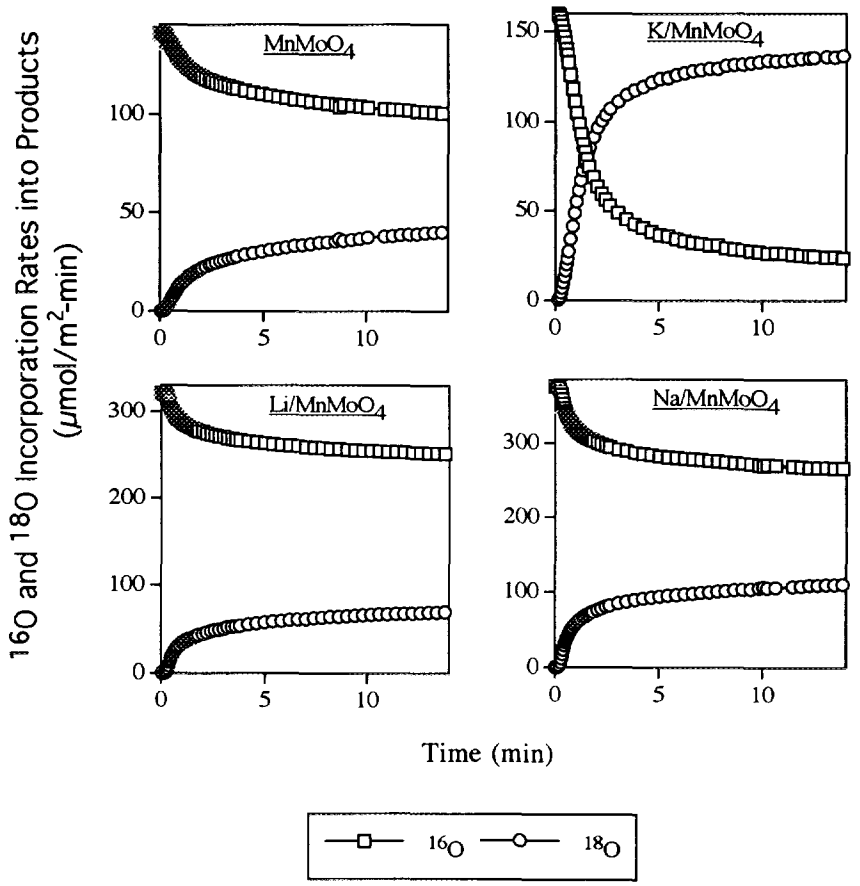

FIG. 14. ^{16}O and ^{18}O incorporation rates into products over unpromoted and alkali-promoted $MnMoO_4$ catalysts.

first interaction with the surface leads to the formation of a partially or completely oxidized product.

Formaldehyde formation is thought to occur through the surface methoxide or peroxide species, a route different from the methyl radical formation leading to gas-phase coupling products (26). Formaldehyde is generally said to decompose at the high temperatures used for the methane coupling reaction, contributing to the production of carbon oxides for oxidative coupling catalysts, and has often been detected only in trace quantities (27). For our system, formaldehyde was formed and detected during the reaction of methane, and the formaldehyde selectivities over Li- and Na-promoted catalysts were significantly higher than that observed over $K/MnMoO_4$. The difference could again be due to the higher oxidation potential of Li- and Na-promoted catalysts, which leads to higher activities for oxygenated species (i.e., CO_x and HCHO) as opposed to coupling products.

TPD experiments performed after CO_2 adsorption indicated that there was no observable interaction between CO_2 and the surface. In addition, the kinetic experiments performed to assess the role of CO_2 on catalytic activity showed no effect on conversion or product distribution. A similar observation has also been reported for the Sm_2O_3 system by Peil *et al.* (18), and it was proposed that the active sites may not serve as significant re-adsorption sites for the product carbon dioxide. This explanation would appear to be the case for our studies, and is supported by our isotopic labeling studies using methane in which the unlabeled carbon dioxide was found to have a very short residence time (24).

At higher levels of oxygen conversion, both Suzuki *et al.* (15) and Aika and Nishiyama (16, 17) observed different behavior for Sm_2O_3. Both groups operated at 100% oxygen conversion and found the addition of carbon dioxide to increase C_2 and CO formation at the expense of CO_2. Part of the explanation may lie in the water gas shift reaction, which would increase the amount of CO through the reaction with hydrogen. As we saw no hydrogen in our product gas analysis, for our experiments this factor would be limited. In fact, there was little change in the calculated catalytic production of CO_2 due to the addition of excess carbon dioxide to the feed.

Results presented in this paper, when combined with our earlier findings (23, 24), provide important clues about the catalytic phenomena that control or affect selectivity

in methane coupling reactions over alkali-promoted simple molybdate catalysts. *In situ* laser Raman spectroscopy studies, which are aimed at examining the catalyst surface under reaction conditions, are currently underway.

ACKNOWLEDGMENTS

The financial support provided by the National Science Foundation through Grant CTS-8912247 is gratefully acknowledged. The authors also acknowledge the assistance of Mr. M. W. Kumthekar and Ms. L. Zhang in laser Raman spectroscopy studies.

REFERENCES

1. Driscoll, S. A., Zhang, L., and Ozkan, U. S., *in* "Catalytic Selective Oxidation" (S. T. Oyama and J. W. Hightower, Eds.), Vol. 523, p. 340. American Chemical Society, Washington, DC, 1993.
2. Keller, G. E., and Bhasin, M. M., *J. Catal.* **73,** 9 (1982).
3. Lo, M.-Y., Agarwal, S. K., and Marcelin, G., *J. Catal.* **112,** 168 (1988).
4. Agarwal, S. K., Migone, R. A., and Marcelin, G., *Appl. Catal.* **53,** 71 (1989).
5. Otsuka, K., Liu, Q., and Morikawa, A., *Inorg. Chim. Acta* **118,** L23 (1986).
6. Otsuka, K., Liu, Q., Hatano, M., and Morikawa, A., *Chem. Lett.*, 467 (1986).
7. Jones, C. A., Leonard, J. J., and Sofranco, J. A., *J. Catal.* **103,** 311 (1987).
8. Iwamatsu, E., Moriyama, N., Takasaki, T., and Aika, K., *in* "Methane Conversion" (D. M. Bibby, C. D. Chang, R. F. Howe, and S. Yurchak, Eds.) p. 373. Elsevier, Amsterdam, 1988.
9. Burch, R., Squire, G. D., and Tsang, S. C., *Appl. Catal.* **43,** 105 (1988).
10. Ito, T., and Lunsford, J. H., *Nature* **314,** 721 (1985).
11. Lin, X.-H., Wang, J.-X., and Lunsford, J. H., *J. Catal.* **111,** 302 (1988).
12. McCarty, J. G., and Quinlan, M. A., *ASC Div. Fuel Chem. Preps.* **33,** 363 (1988).
13. Korf, S. J., Roos, J. A., DeBruijn, N. A., Van Ommen, J. G., and Ross, J. R. H., *Appl. Catal.* **58,** 131 (1990).
14. Hutchings, G., Scurrell, M. S., and Woodhouse, J. R., *Catal. Today* **6,** 399 (1990).
15. Suzuki, T., Wada, K., and Watuabe, Y., *Appl. Catal.* **59,** 213 (1990).
16. Aika, K., and Nishiyama, T., *in* "Proceedings, 9th International Congress on Catalysis, Calgary, 1988" (M. J. Phillips and M. Ternan, eds.), Vol. 2, p. 907. Chem. Institute of Canada, Ottawa, 1988.
17. Aika, K., and Nishiyama, T., *J. Chem. Soc., Chem. Commun.*, 70 (1988).
18. Peil, K. P., Goodwin, J. G., Jr., and Marcelin, G., *in* "Natural Gas Conversion" (A. Holmen *et al.*, Eds.), p. 73. Elsevier, Amsterdam, 1991.
19. Roos, J. A., Korf, S. J., Veehof, R. H. J., Van Ommen, J. G., and Ross, J. R. H., *Appl. Catal.* **52,** 131 (1989).
20. Nishiyama, T., and Aika, K., *J. Catal.* **122,** 346 (1990).
21. Kiwi, J., Thampi, K. R., Gratzel, M., *J. Chem. Soc., Chem. Commun.*, 1690 (1990).
22. Carreiro, J. A. S. P., Follmer, G., Lehmann, L., Baerns, M. *in* "Proceedings, 9th International Congress on Catalysis, Calgary, 1988" (M. J. Phillips, and M. Ternan, Eds.), Vol. 2, p. 891. Chem. Institute of Canada, Ottawa, 1988.
23. Driscoll, S. A., and Ozkan, U. S., *J. Phys. Chem.* **97** (44), 11524 (1993).
24. Driscoll, S. A., Gardner, D. K., and Ozkan, U. S., to be published in *Catal. Lett.*
25. Ozkan, U. S., Gill, R. C., and Smith, M. R., *J. Catal.* **116,** 171 (1989).
26. Peng, X. D., and Stair, P. C., *J. Catal.* **128,** 264 (1991).
27. MacGiolla Coda, E., and Hodnett, B. K., *in* "New Developments in Selective Oxidation" (G. Centi, and F. Trifiro, Eds.), p. 45. Elsevier, Amsterdam, 1990.
28. Colthup, N. B., Daly, L. H., and Wilberley, S. E., *in* "Infrared and Raman Spectroscopy." Academic Press, New York, 1990.